ACS OMEGA

http://pubs.acs.org/journal/acsodf

Article

An Organometallic Flame Retardant Containing P/N/S−Cu^{2+} for Epoxy Resins with Reduced Fire Hazard and Smoke Toxicity

Junwei Li, Penglun Zheng,* Huaiyin Liu, Jichang Sun, Yawei Meng, Haihan Zhao, Jing Wu, Yun Zheng,* and Quanyi Liu*

Cite This: *ACS Omega* 2023, 8, 16080−16093

Read Online

ACCESS | Metrics & More | Article Recommendations

ABSTRACT: Epoxy resins (EPs) have superior physical and chemical features and are used in a wide range of applications in everyday life and engineering. However, its poor flame-retardant performance has hindered its wide application. Over the past decades of extensive research, metal ions have received increasing attention for their highly effective smoke suppression properties. In this work, we used an "aldol-ammonia condensation" reaction to structure the Schiff base structure, together with grafting using the reactive group on 9,10-dihydro-9-oxa-10-phospha-10-oxide (DOPO). Then, Cu^{2+} was used to replace Na^{+} to obtain DCSA-Cu flame retardant with smoke suppression properties. Attractively, DOPO and Cu^{2+} can collaborate, thus effectively improving EP fire safety. At the same time, the addition of a double-bond initiator at low temperatures allows small molecules to form in situ macromolecular chains through the EP network, enhancing the tightness of the EP matrix. With the addition of 5 wt % flame retardant, the EP shows well-defined fire resistance, and the limiting oxygen index (LOI) reaches 36% with a significant reduction in the values of peak heat release (29.72%). In addition, the glass-transition temperature (T_g) of the samples with in situ formations of macromolecular chains was improved, and the physical properties of EP materials are also retained.

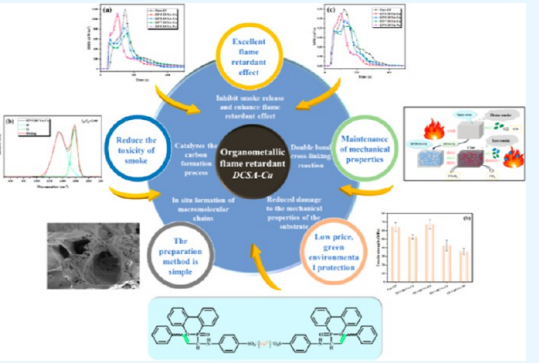

1. INTRODUCTION

Epoxy resins (EPs) are used extensively in the industry for their excellent physical and chemical properties, such as superior adhesion, sealing, heat resistance, and chemical resistance.[1−3] However, due to its inherent flammability and it generates a lot of smoke and heat from burning will greatly limit the scope of pure EP in practical applications. Recently, a wide variety of methods have been put forward to enhance the flame retardancy of EP. The most common method is through the addition of flame retardants. Halogen-containing flame retardants are the earliest additive flame retardants used on a large scale, but their combustion produces large amounts of acidic and toxic gases as well as produce permanent pollutants that will damage the environment.[4,5] Therefore, halogen flame retardants are progressively eliminated from industrial applications. The halogen-free flame retardants have been widely concerned.

The most commonly used halogen-free flame retardants include phosphorus-based flame retardants, nitrogen-based flame retardants, silicon-based flame retardants,[6] metal hydroxides (such as magnesium hydroxide and aluminum hydroxide), boron-containing compounds (such as boric acid and borax), etc. Phosphorus-based flame retardants are regarded as high-efficiency flame retardants due to their efficient fire-retardant properties.[7−9] Among the phosphorous compounds, especially those containing 9-10-dihydro-9-oxa-10-phosphaphenanthrene-10-oxide (DOPO), their derivatives exhibit excellent flame retardant.[10,11] Nitrogenous complexes may be used alone as flame retardants or as additives to other fire retardants (e.g, phosphorus)[12−14] to enhance their activity. Though these phosphorus and nitrogen organic flame retardants can effectively enhance the flame-retardant performance of EP, they have less effect on the release of smoke during the burning of EP. Metal oxides and their hydroxides[15] can be used as inorganic flame retardants to effectively improve the smoke suppression performance of polymeric materials,[16−18] but owing to their low flame-retardant efficiency, it has to be added in large quantities[19] to obtain the fireproof effect, which seriously damages the mechanical properties of polymeric materials.[20] Much research has been conducted to show that the combination of metal ions introduced into flame retardants

Received: December 27, 2022
Accepted: April 19, 2023
Published: April 27, 2023

Scheme 1. Synthesis Routine of DCSA-Na

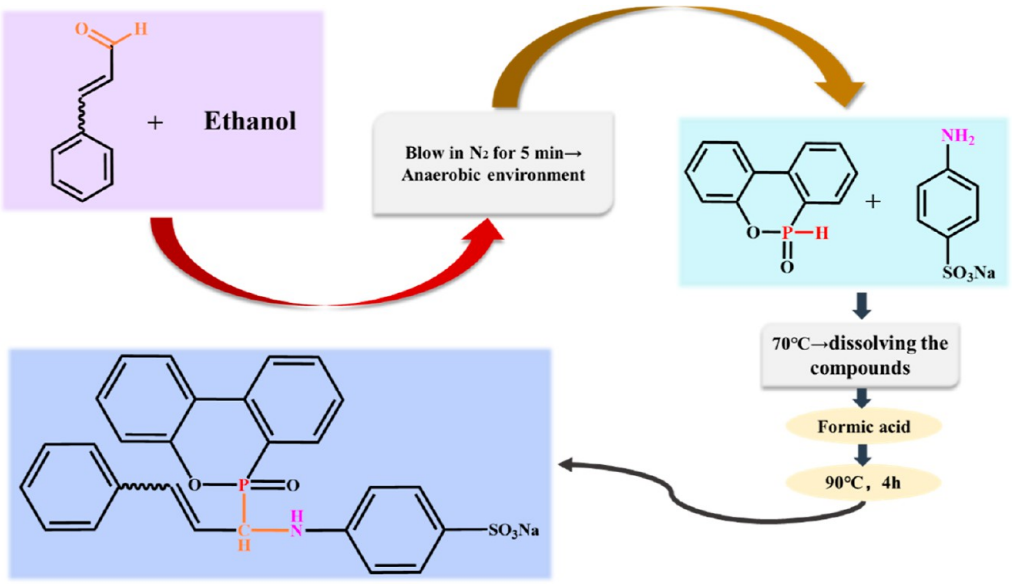

Scheme 2. Synthesis Routine of DCSA-Cu

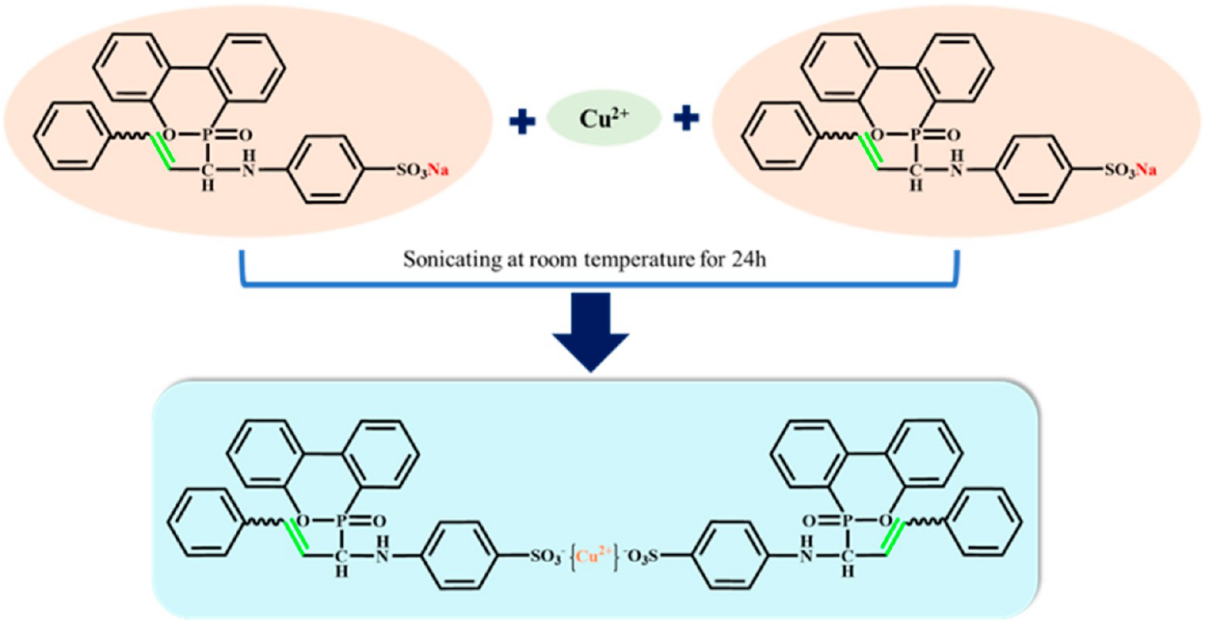

can successfully reduce the smoke emissions from the burning of compound materials[21−24] and catalyze the conversion of toxic gases, significantly reducing environmental pollution. Metal organic framework and other carbon-forming agents for synergy can promote the matrix into carbon,[25] protect the matrix from further combustion, and enhance the flame-retardant properties of the composite. At the same time, the metal oxides have significant suppression of flue gas and toxic gases.[26,27] The introduction of some metal ions requires grafting reactions, in situ growth, synthesis of organometallic frameworks, etc. Although they can achieve good flame-retardant and smoke suppression effects through the joint action of organic ligands and metal ions, they have problems such as complex reactions and more difficult preparation.

Due to the foregoing analysis and being combined with previous work carried out in our laboratory on the preparation of cross-linked flame retardants,[28−30] we designed and prepared a phosphorus-containing flame retardant with both double bonds and metal ions. It is well known that added flame retardants generally affect other properties of the matrix,[31,32] and it is worth noting that the DCSA-Cu flame retardants in this study are prepared by simple mutual attraction of charges between anions and cations and the replacement of metal ions, which is a less difficult and simple method. At the same time, the double-bond structure contained in the flame retardant itself can form a macromolecular chain structure in situ and maintain the mechanical properties of the composite material. In summary, the impact of DCSA-Cu on flame retardancy and the thermal and mechanical properties of EP were investigated methodically in this paper, and the basic flame-retardant mechanics was also been described.

https://doi.org/10.1021/acsomega.2c08226
ACS Omega 2023, 8, 16080−16093

2. EXPERIMENTAL SECTION

2.1. Materials. The diglycidyl ether of biphenol-A epoxy resin (E51, epoxide equivalent of 0.51 eq/100 g) was obtained from Shandong Xinkai Chemical Co., Ltd., China. The 4,4′-diaminodiphenylmethane (DDM) was purchased from Shanghai Energy Chemical Co., Ltd., China. Cinnamaldehyde, ethanol, formic acid, DOPO, sodium *p*-aminobenzenesulfonate(SA-Na), and copper (II) sulfate pentahydrate ($CuSO_4{\cdot}5H_2O$) were purchased from Adamas. All the reagents were used on their own without any additional purification. All experiments were conducted with deionized water unless otherwise stated.

2.2. Sample Synthesis. The synthesis reaction of DCSA-Na is shown in Scheme 1. A mixture of cinnamaldehyde (100 mmol) is added in ethanol, nitrogen gas is then introduced and held for 5 min, and DOPO (100 mmol) and SA-Na (100 mmol) are added. The reaction temperature is then increased to 70 °C for dissolution. When the dissolution is complete, the formic acid is added dropwise, the temperature is ascended to 90 °C, and the reaction process is maintained for 6 h. After the reaction, it was washed with alcohol several times. At last, the alcohol was removed in the vacuum oven at 80 °C for 12 h, and the light yellow solid was crushed to obtain the DCSA-Na white powder (DCSA-Na, yield: 92%).

The synthesis reaction of DCSA-Cu is shown in Scheme 2. The obtained DCSA-Na powder was added into the 0.1 mol/L copper sulfate solution prepared in advance and sonicated for 36 h at ambient temperature to make the copper ions completely replace the sodium ions, then centrifuged and cleaned with deionized aqueous water several times and to eliminate water in an evaporator for drying oven at 100 °C for 30 h, and the earthy yellow solid received was ground to obtain DCSA-Cu yellow powder (DCSA-Cu, yield: 87.5%).

2.3. Curing EP Sample Fabrication. The DDM is adopted as the sole curing factor for E51, and DCSA-Na and DCSA-Cu are used as the fire retardants for E51; the weights of E51, DDM, and the fire retardants are shown in Table 1.

Table 1. Formulas of Epoxy Thermosets

samples	E51 (wt %)	DDM (wt %)	DCSA-Cu/Na (wt %)	content of P (wt %)
pure EP	80.0	20.0	0	0
EP/3-DCSA-Cu	77.6	19.4	3	0.16
EP/5-DCSA-Cu	75.9	19.1	5	0.27
EP/7-DCSA-Cu	74.4	18.6	7	0.38
EP/5-DCSA-Na	75.9	19.1	5	0.28

A pure sample of EP was made by the following physical methods: agitating E51 in an oil bath at 120 °C to obtain E51 in a form similar to that of water. After the temperature was lowered to below 75 °C and DDM was added, the DDM was dissolved in E51, then the mixture was put into a vacuum oven at 60 °C to remove the bubbles, and the mixture was poured into the Teflon mold. Finally, the mixture is first cured in a vacuum oven at 120 °C for 2 h, followed by a blowing oven at 150 °C for 2 h, and finally, the mixture is cured at 180 °C for 2 h.

The EP/DCSA-Cu and EP/DCSA-Na samples were prepared by the same physical process as pure EP samples: first E51 was stirred in an oil bath set at 120 °C, and DCSA-Cu (Na) was added. Then, the temperature was lowered to below 75 °C, and DDM was added. While the DDM was dissolved in E51, a quantitative amount of the double-bond initiator was also added, then the mixture was put into a vacuum oven at 60 °C to remove air bubbles, and the mixture was poured into the Teflon mold. Finally, the mixture was first cured in a vacuum oven at 120 °C for 2 h, then in a blown oven at 150 °C for 2 h, and finally at 180 °C for 2 h.

3. RESULTS AND DISCUSSION

3.1. Structural Characteristics of Flame Retardants. ^{1}H NMR, ^{31}P NMR, and FTIR were used to symbolize the flame retardants. As illustrated in Figure 1a, the P−H, P−Ph, P═O, and P−O−Ph stretching vibrations of the DOPO are allocated to the characteristic peaks at 2441, 1427, 1232, and 901 cm^{-1}.[28] In the spectrum of cinnamaldehyde, the peak of 2815 cm^{-1} is −CHO, and the characteristic absorption peak of C═C is detected at 1623 cm^{-1} as the same as the spikes detected at 1600 cm^{-1} in the spectrum of DCSA-Na. In the SA-Na spectrum, the double peaks at 3331 and 3378 cm^{-1} were attributed to $-NH_2$. Finally, the $-NH_2$, P−H, and −CHO peaks disappeared, the C═C (1600 cm^{-1}), P═O (1231 cm^{-1}), P−Ph (1427 cm^{-1}), P−O−Ph (924 cm^{-1}) peaks sustained, and the on indication of N−H (1585 cm^{-1}), C−N (1447 cm^{-1}), and P−C peaks,[29] the DCSA-Na was confirmed to have been successfully composite. As indicated in Figure 1b, a comparison of the FTIR spectra of DCSA-Na and DCSA-Cu shows that DCSA-Cu possesses all the characteristic functional groups of DCSA-Na. This is because their structures are identical and differ only in the metal ion ligands. Since the N−H bond also exists in the final product DCSA-Cu, it also shows a corresponding characteristic peak at 3303 cm^{-1}, while Cu^{2+} attracts two sulfonic acid groups, so it shows a fluctuating characteristic peak at 3303−3500 cm^{-1}.

To further confirm the synthesized structure, the ^{1}H NMR and ^{31}P NMR of DCSA-H (which is obtained by immersing DCSA-Na in a certain concentration of acid, mainly for the convenience of dissolving in the solvent for NMR) were also considered. The ^{1}H NMR spectrogram of DCSA-H is illustrated in Figure 1c, except for the DMSO (2.5 ppm) peak, the chemical shifts from 6.88 to 8.12 ppm show peaks attributed to the aromatic hydrogen atoms of the benzene ring in DCSA-H. The signal has been surveyed at 9.47 ppm corresponding to the $-SO_3H$ proton. The proton peak of −C═C− appears at 5.35−5.65 ppm. The peak of the C−H group between phosphorus and nitrogen occurs at 5.82 ppm, while the peak at 6.54 ppm is attributed to the hydrogen atom in the N−H bond. Furthermore, the integral area ratio (from C−H, N−H, benzene, and $-SO_3H$) is 3:1:17:1, which is very close to the DCSA-H chemistry. Moreover, in the ^{31}P NMR spectra of DOPO, the peaks of phosphorus atoms generally appeared at 15.76 and 13.24 ppm,[28] but the ^{31}P NMR spectra of DCSA-H (Figure 1d) showed that there are two high points at 31.51 and 36.86 ppm, which did not correlate to the DOPO peaks, which meant that DOPO had been successfully reacted and broken into DCSA-H. Therefore, the NMR results further demonstrate the synthesis of DCSA-H according to the design.

The SEM image of the DCSA-Cu is shown in Figure 2a. To further confirm the synthesis of DCSA-Cu, an energy-dispersive EDX spectroscope was used to illustrate it, and the result is shown in Figure 2g. It is known that there are C, N, O, P, S, and Cu elements. This effectively proves the presence of copper elements in the DCSA-Cu flame retardant.

3.2. Curing Behaviors. DCSA-Na and DCSA-Cu were synthesized according to the process conditions in Schemes 1

https://doi.org/10.1021/acsomega.2c08226
ACS Omega 2023, 8, 16080−16093

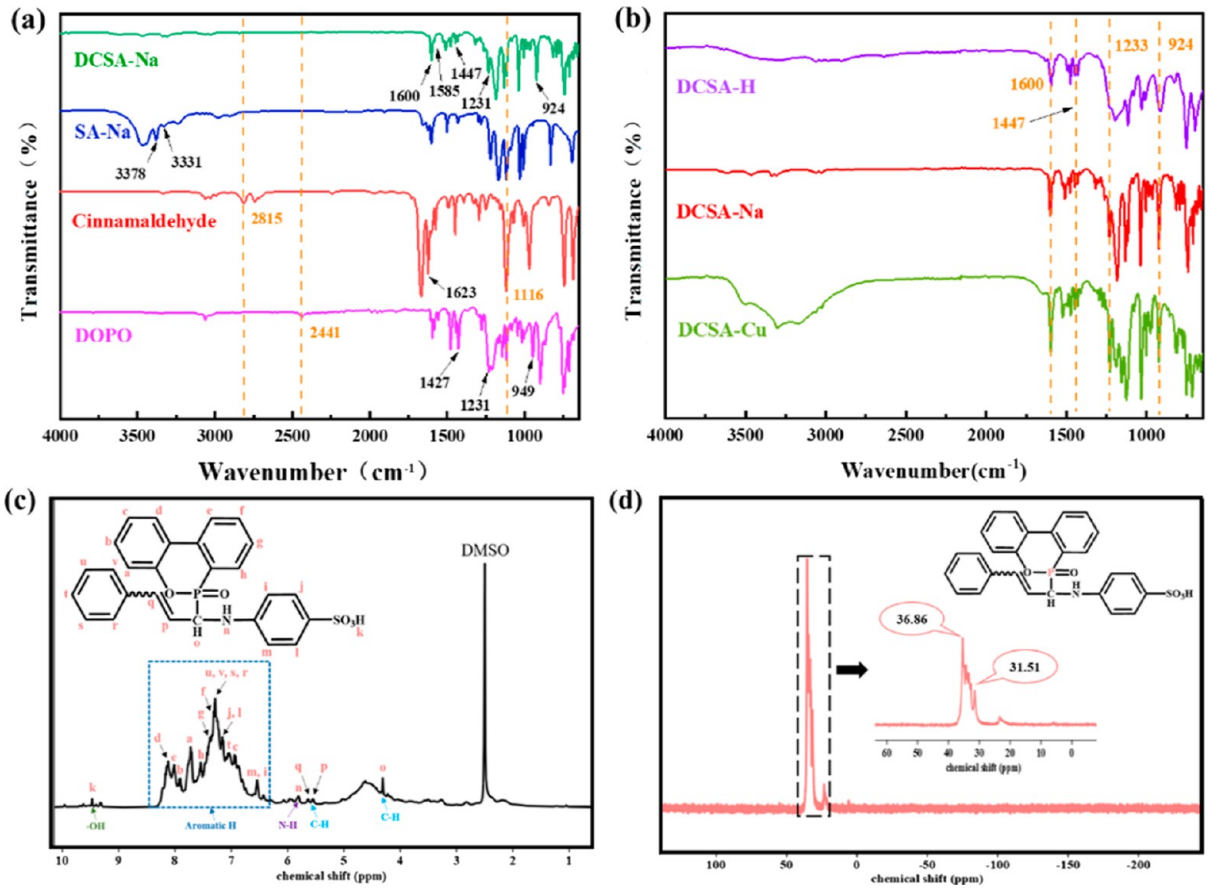

Figure 1. FTIR spectra of DOPO, cinnamaldehyde, SA-Na, and DCSA-Na (a), spectra of DCSA-H, DCSA-Na, and DCSA-Cu (b), and ^{1}H NMR (c) and ^{31}P NMR (d) spectrum of DCSA-H.

and 2, respectively, and the modified specimens were obtained by the mechanical stirring process. To confirm the curing behaviors of the DCSA-Na (Cu) mixed EP composites, DSC was used, and the spectra are shown in Figure 3. All samples show only one exothermic peak, which corresponds to the curing reaction of EP. In addition, it was found that the curing peak of EP as a whole shifted toward the low-temperature region with the addition of DCSA-Na (Cu). The curing exothermic peak of 5 wt % loading of DCSA-Cu occurs at 146 °C, which was a 14 °C decrease from pure EP. This suggests that the DCSA-Na (Cu) may facilitate the curing reaction of EP because the remaining N−H bond after the Schiff base reaction can facilitate the curing of EP, and the presence of the metal ions can be used as an effective catalyst to facilitate the curing process of EP.[15] It can be seen from Figure 3b that irrespective of the addition of DCSA-Cu or DCSA-Na, they have less effect on the overall curing process of the EP due to their lesser addition. In general, the addition of a small amount of DCSA-Cu to the epoxy matrix has a little effect on the curing process.

3.3. Thermal Stability of the EP Thermosets. Thermal stability analysis of EP composites was carried out using TGA. Figure 4 shows the TG and DTG curves of EP composites. The key parameters, which can be obtained from the curves shown in Table 2, are 5% by weight loss ($T_{5\%}$), maximum mass loss rate (T_{max}), peak DTG curve (D_{max}), and residue char at 700 °C (C_{y700}). Pure EP exhibits only one degradation process, which occurs between 370 and 540 °C, and it corresponds to the breakage of the EP molecular lattice. The TG curves have revealed that the EP composites show mainly one degradation process in the nitrogen environment, which is similar to the decomposition process of pure EP. The $T_{5\%}$ of all composites is lower than the $T_{5\%}$ of pure EP, especially for EP/7-DCSA-Cu composites. It is interesting to note that in Figure 4a, pure EP and EP/5-DCSA-Na composites have almost the same residual weight, suggesting that the DCSA-Na has not much impact on EP char-formation. DOPO usually plays a huge role in gas phase flame retardation,[33,34] and the Na^{+} is unable to catalyze the carbon formation process of EP, which results in a low residual amount of EP/DCSA-Na composites. Nevertheless, the high mass of residue after the combustion of EP/DCSA-Cu composites is mainly attributed to Cu^{2+} blocking and catalysis. It is recommended to note that the increase of the Cu^{2+} content makes the final residual weight increase as well. In theory, the DOPO can inhibit flame formation in the gas phase, and the Cu^{2+} oxide exhibits a barrier and a catalyst effect to block the heat transfer and promote the formation of char.[35] Therefore, the gas-phase flame retardancy of DOPO and the synergistic effect of Cu^{2+}-catalyzed carbon formation in the epoxy matrix could significantly strengthen the flame retardancy of composite materials. It was demonstrated that transition metals probably catalyze the early degradation of EP composites.[36] So, compared with pure EP, the degradation process was accelerated in EP/DCSA-Cu groups.

Moreover, the DTG curves showed that the greatest breakdown rate of the epoxy-cured resin decreased with the addition of DCSA-Cu, denoting that the addition of DCSA-Cu inhibits the thermal decomposition of the epoxy curing

https://doi.org/10.1021/acsomega.2c08226
ACS Omega 2023, 8, 16080−16093

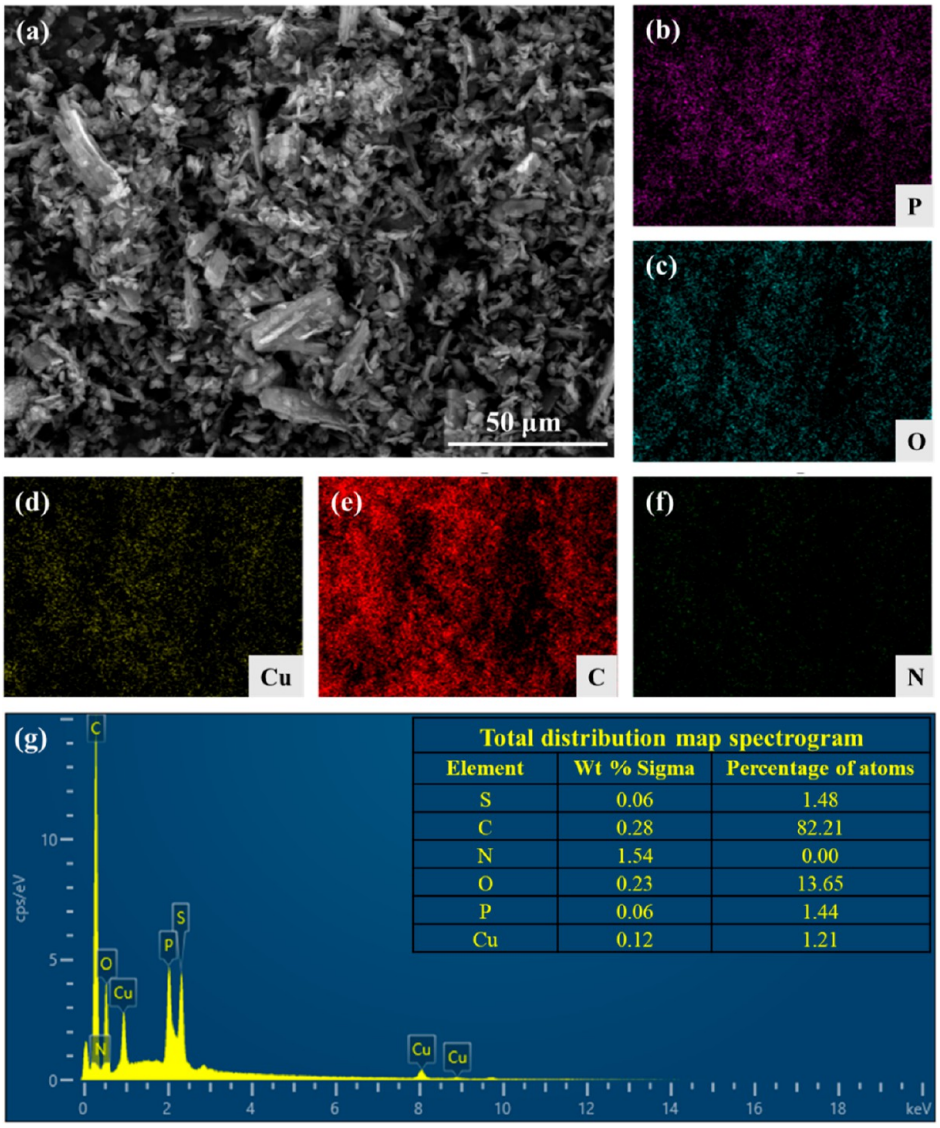

Figure 2. SEM images of DCSA-Cu (a) and corresponding element mapping of P (b), O (c), Cu (d), C (e), and N (f); and EDX results of DCSA-Cu (g).

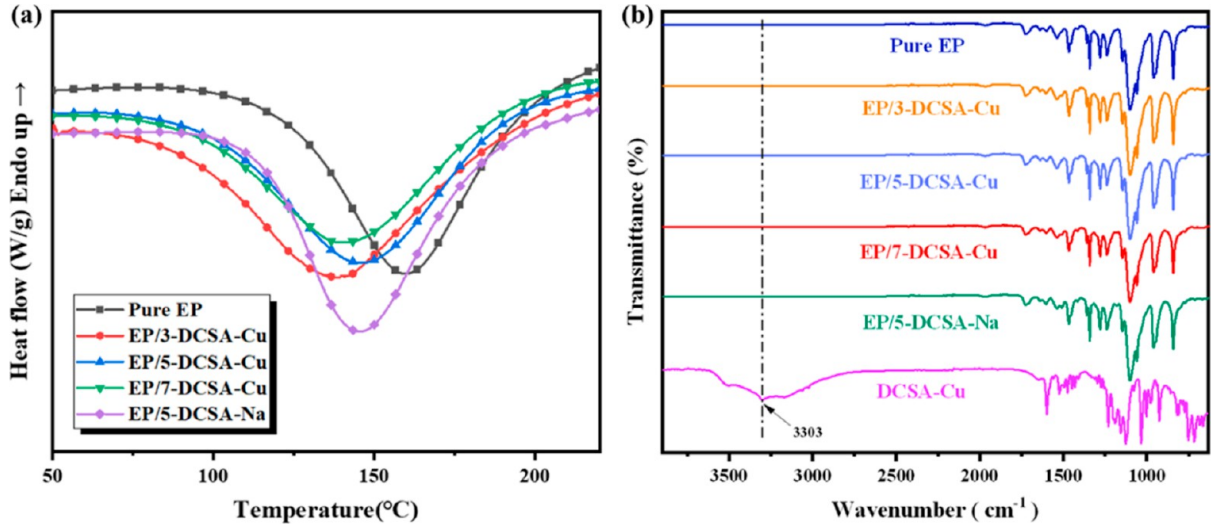

Figure 3. DSC curves of EP composites (a); FTIR spectra of pure EP, EP/3-DCSA-Cu, EP/5-DCSA-Cu, EP/7-DCSA-Cu, EP/5-DCSA-Na, and DCSA-Cu (b).

https://doi.org/10.1021/acsomega.2c08226
ACS Omega 2023, 8, 16080−16093

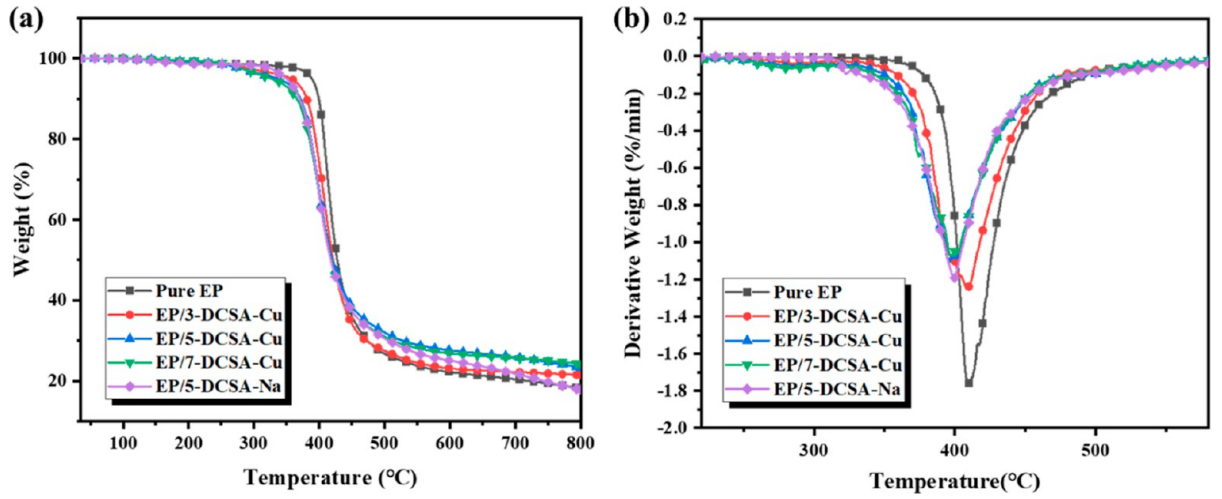

Figure 4. TGA (a) and DTG (b) curves of pure EP and EP composites in N_2.

Table 2. TGA Data of EP Composites

sample	$T_{5\%}$(°C)	T_{max}(°C)	D_{max}(%/°C)	C_{y700}(%)
Pure EP	388.5	409.8	−1.77	20.4
EP/3-DCSA-Cu	353.0	408.0	−1.24	24.2
EP/5-DCSA-Cu	326.1	394.2	−1.10	24.7
EP/7-DCSA-Cu	326.5	395.1	−1.11	25.7
EP/5-DCSA-Na	348.6	399.2	−1.13	21.3

compound in the high-temperature region. This may be due to the catalytic carbon formation by metal ions.

3.4. Dynamic Mechanical Properties of Cured EP. Generally, T_g is employed to characterize the difficulty of moving polymer chains at high temperatures, which is influenced by factors such as packing, cross-link density, cross-sectional freedom, and wound degree. T_g of EP and its composites are illustrated in Figure 5. The results show that there is only one transition peak on the loss factor curve, which shows that the additive is compatible with EP. Furthermore, the T_g of EP composites is higher than pure EP because of the stronger entangling force of the modified molecular chains. Interestingly, the composites of the EP/DCSA-Cu group all have higher T_g than those of EP/5-DCSA-Na because Cu^{2+} can act as a bridge between the molecular chains to form a denser structure, whereas Na^+ can only form a single molecular chain, which leads to poorer entanglement.

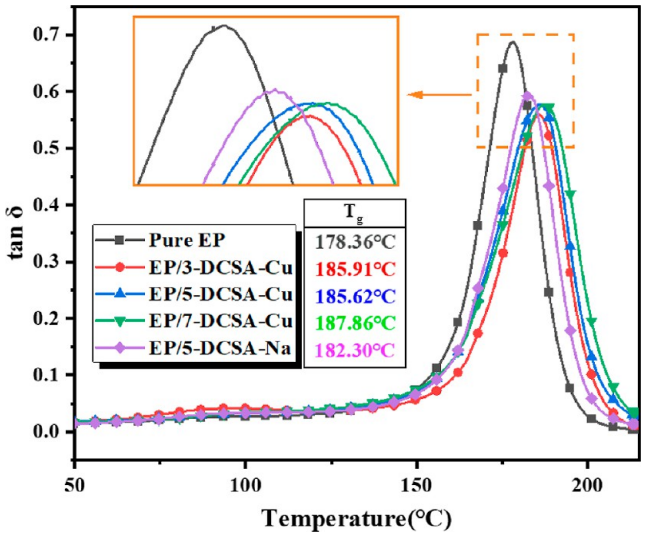

Figure 5. Tan δ curves of EP and its composites.

In summary, whether DCSA-Cu or DCSA-Na is added, the large molecular chains formed in situ by double bonds between the molecules can further confer better heat resistance to the modified EP composites, which means that this flame-retardant reaction method will remain thermally stable.

3.5. Fire Performances. The fire resistance of EP composites was tested using LOI and UL-94 methods. The performance is displayed in Table 3 and Figure 6. Pure EP is extremely flammable in the air with an LOI of 26% and fails UL-94 testing, but the addition of a small amount of Cu^{2+} has improved the flame-retardant characteristics of the EP matrix significantly, with an LOI of 33.3% for the DCSA-Cu composite of 3 wt %. With only 5 wt % of DCSA-Cu added, EP/5-DCSA-Cu reached the ratio of UL-94V-0 with no decrease, and the LOI value reached 36%, which shows that DCSA-Cu is a functional flame retardant. As the DCSA-Cu content increases, the LOI values first increase and then decrease. This is because high additions of flame retardants cause intermolecular agglomeration, which can lead to a decrease in the LOI of EP/7-DCSA-Cu composites. Yet, the addition of DCSA-Na had little effect on the LOI value (29.5%), which is due to the small effect of Na^+ on the flame-retardant properties of the EP matrix.

Table 3. Flammability Test Results of Flame-Retardant Epoxy Thermosets

		UL-94 burning test		
samples	LOI (%)	$t_1 + t_2$ (s)	dropping	rate
pure EP	26.0	>180	yes	no rate
EP/3-DCSA-Cu	33.3	28	no	V-1
EP/5-DCSA-Cu	36.0	8	no	V-0
EP/7-DCSA-Cu	32.2	25	no	V-1
EP/5-DCSA-Na	29.5	32	no	V-1

The bulk of fire fatalities result from heat exposure, smoke inhalation, and CO suffocation. So, these three factors are of great importance for the safety assessment of the flame-retardant polymer. The cone calorimeter test is a precise

https://doi.org/10.1021/acsomega.2c08226
ACS Omega 2023, 8, 16080−16093

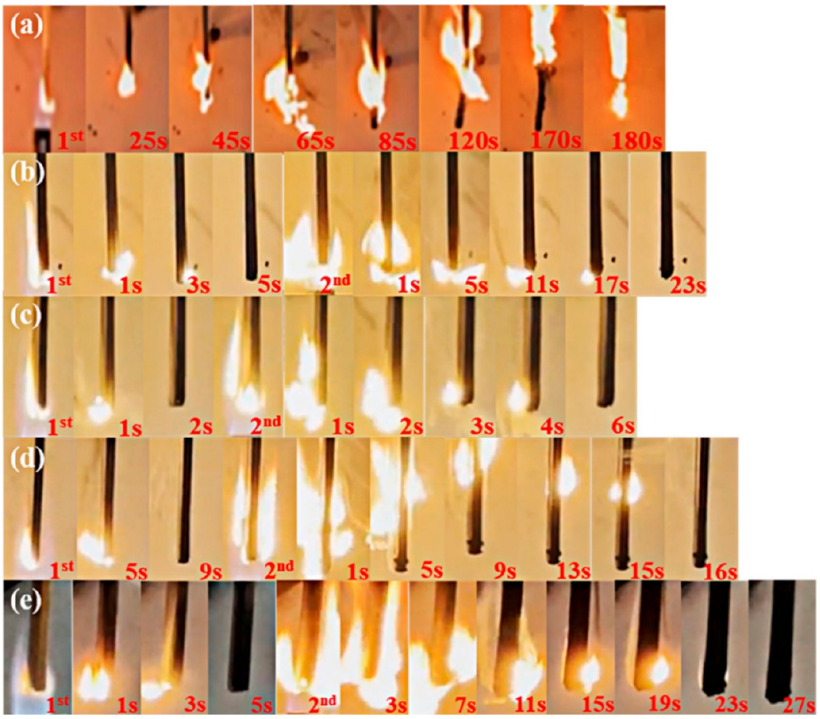

Figure 6. Video screenshots of the modified samples in the UL-94 test. (a) Pure EP; (b) EP/3-DCSA-Cu; (c) EP/5-DCSA-Cu; (d) EP/7-DCSA-Cu; and (e) EP/5-DCSA-Na.

Table 4. Cone Calorimetric Parameters of EP and EP Composites

samples	pure EP	EP/3-DCSA-Cu	EP/5-DCSA-Cu	EP/7-DCSA-Cu	EP/5-DCSA-Na
TTI (s)	46	42	43	43	41
THR ($MJ·m^{-2}$)	158.0	135.6	130.6	138.3	138.7
PHRR ($kW·m^{-2}$)	1204.4	1081.2	846.5	708.8	1126.7
t_{PHRR} (s)	102	62	104	116	64
TSP (m^2)	40.6	27.8	34.8	35.8	29.1
PSPR ($m^2·s^{-1}$)	0.34	0.33	0.28	0.33	0.31
t_{PSPR} (s)	130	108	128	46	96
TSR (m^2/m^2)	4561.2	3121.3	3898.6	3991.4	3237.9

method for analyzing the fire resistance of composite polymers. Full data for the cone calorimetry experiment are presented in Table 4. Based on these parameters, it is possible to get the burning condition and performance of the combustion process, such as time to ignitio (TTI), peak heat release rate (PHRR), total heat release rate (THR), TSP, peak smoke generation rate (PSPR), and total smoke release (TSR).

The TTI for pure EP was 46 s, but the addition of DCSA-Cu and DCSA-Na resulted in a lower TTI for both composites. For the 5 wt % DCSA-Cu loading, the TTI was 43 s, suggesting that DCSA-Cu could advance the decomposition, and the deterioration of EP has been accentuated, which corresponds to the results of TGA. The PHRR and THR can be used to investigate composite material heat release process and fire resistance. As shown in Figure 7a,b, the values of PHRR and THR decreased with the addition of the two flame retardants. The results showed that EP/5-DCSA-Cu could decrease the PHRR and THR values (more than 29.72 and 17.3% decreases, respectively), which is greater than EP/5-DCSA-Na, and it is shown that DOPO and Cu^{2+} have a co-operative function in heat release reduction. DOPO in the gas phase prevents the spread of fire, which means less heat is transferred to the EP matrix. Furthermore, Cu^{2+} catalyzes the carbon formation process of the EP substrate, and the resulting oxide acts as a barrier to cover the surface of the carbon layer.[37,38]

The smoke evacuation performance of polymers is an important factor in evaluating their fire resistance. In a fire, the smoke obscures people's view and also tends to cause asphyxiation. As seen in Figure 7c, the additive significantly inhibited the release of smoke. At the same time, the PSPR was decreased, and the time of EP/5-DCSA-Cu to PSPR was not delayed, but PSPR has decreased, which meant that the smoke emission was suppressed. The PSPR reduction for EP/5-DCSA-Cu was 17.65%, suggesting an excellent smoke suppression performance for the DCSA-Cu. The peak time for the EP/5-DCSA-Na composites was earlier due to the pre-gas phase action of DOPO, and the peak time for the EP/3-DCSA-Cu composites was also earlier because the catalytic carbon formation of the low Cu^{2+} content was less than the pre-gas phase action of DOPO.

In addition, as shown in Figure 7d, the TSP increases with the increasing DCSA-Cu content, which may be due to the increased DOPO content pre-driving the release of more gas, increasing total smoke production. The release rates of CO and CO_2 are shown in Figure 7e,f. The findings implied that the

https://doi.org/10.1021/acsomega.2c08226
ACS Omega 2023, 8, 16080−16093

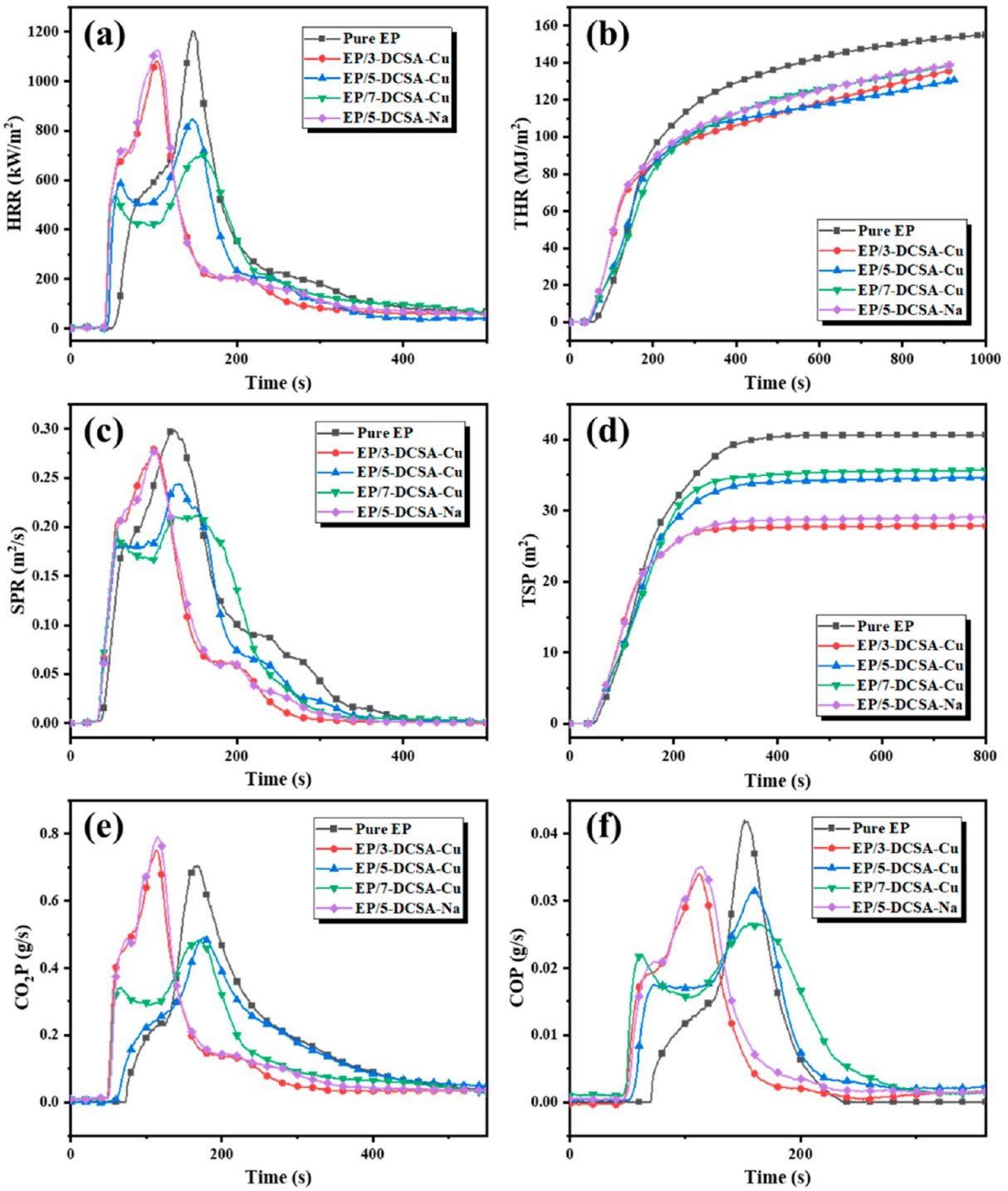

Figure 7. HRR (a), THR (b), SPR (c), TSP (d), CO_2P (e), and COP (f) curves versus time for EP composites.

addition of 5% DCSA-Na had a less inhibitory effect on the release of CO. When 5 and 7% of DCSA-Cu were added, it significantly delayed the peak of CO release and produced a significant depression of CO. This observation suggests that in the case of DCSA-Cu hybrids containing EP compounds, more time is required to achieve a lethal concentration of CO. The flame retardant itself contains transition-metal elements that will further catalyze the carbon formation process of EP, while the combination with copper oxides will rapidly form a gas and thermal barrier, thus delaying the release of smoke.

3.6. TG-FTIR Analysis. During the burnout of EP composites, their combustion products can have a great influence on flame increase and diffusion. The introduction of a flame retardant will reduce the concentration of combustible gases produced by combustion and thus suppresses the burning of the matrix of the polymer. To investigate the mechanism of the DCSA-Cu flame retardant to EP, the thermal decomposition products of the EP-cured samples were investigated by TG-IR tests under different temperature conditions in a nitrogen atmosphere. Figure 8 represents the IR spectra of the thermal decomposition products of pure EP

https://doi.org/10.1021/acsomega.2c08226
ACS Omega 2023, 8, 16080−16093

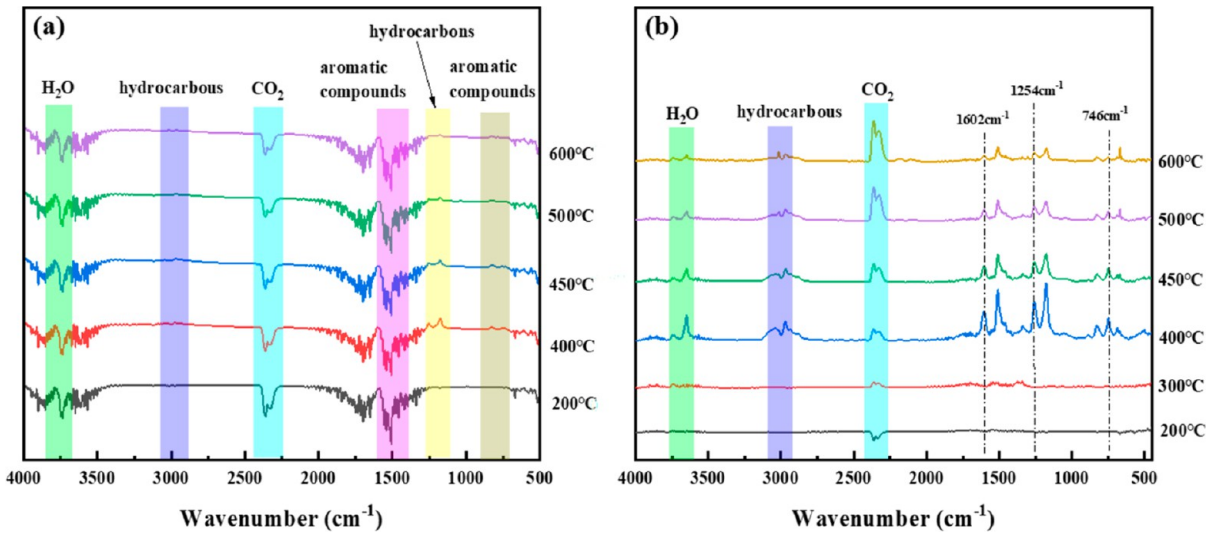

Figure 8. IR spectra of gas products at different temperatures: pure EP (a) and EP/5-DCSA-Cu (b).

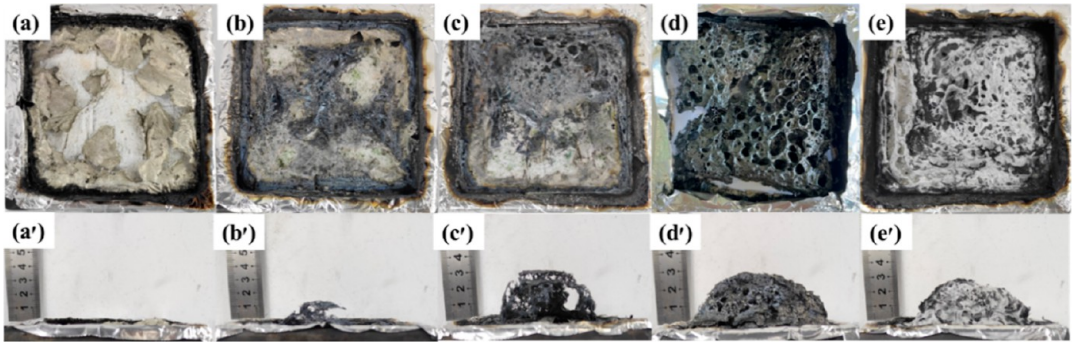

Figure 9. Digital photographs of char residues from CCT. Pure EP (a and a'); EP/3-DCSA-Cu (b and b'); EP/5-DCSA-Cu (c and c'); EP/7-DCSA-Cu (d and d'); and EP/5-DCSA-Na (e and e').

and EP/5-DCSA-Cu at different temperatures. The key production of EP decomposition consisted of C−O (1254 cm^{-1}) and C−H (1337 and 1180 cm^{-1}) of bisphenol A and CO_2 (2378 cm^{-1}) and C−H of aromatic hydrocarbons (3041, 1511, 1601, and 828 cm^{-1}) and aliphatic compounds (2862−3104 cm^{-1}). In comparison to EP, no new peaks appeared in the EP/5-DCSA-Cu spectrum. Remarkable changes in peak intensities can be detected. For instance, the peak at 1254 cm^{-1} (P═O) overlaps with the feature C−O and C−H peaks of BPA, which results in an additional peak height. The increased peak at 746 cm^{-1} is due to the presence of DOPO. The above results indicate that products containing multiple phosphates were formed during the thermal decomposition of the EP/DCSA-Cu composites. In addition, the complexes of compounds containing polyphosphate structures reacted with other decomposition products during disintegration to form P−O-Ph (1602 cm^{-1}) bonds.

3.7. Morphology of the Char Residue. The characteristics of char residues, such as weight, graphitization degree, and micro-topography, have been frequently used to describe the effect of agents on the char-generation reaction.

As evidenced by the digitized images in Figure 9, the pure EP composites have almost no carbon slag generation, and EP/5-DCSA-Na composites have only a small amount of carbon slag generation. The composites of the EP/DCSA-Cu group all produced charcoal residue after combustion, and this increased with increasing addition, which is good evidence of the catalytic carbon formation of Cu^{2+}. Interestingly, the EP/5-DCSA-Cu composite can already form a solid carbon formation after combustion, while the EP/7-DCSA-Cu composite forms more dense layer after combustion, probably due to the increase in Cu^{2+} making the catalytic carbon formation stronger. Also, the degree of graphitization of the carbon slag can be studied by Raman spectroscopy. As shown in Figure 10, pure EP has the highest I_D/I_G value, while EP/5-DCSA-Cu has the lowest I_D/I_G value, indicating that the carbon slag of EP/5-DCSA-Cu has a higher degree of graphitization and therefore can effectively prevent heat transfer, thus raising the fire resistance of composite materials.

The microscopic morphology of the carbon residue was observed by SEM, as shown in Figure 11. The powdered carbon residues of the pure EP and EP/DCSA-Na composites are carbon particles of different sizes. With the addition of DCSA-Cu, a continuous carbon layer appeared in the field of view, but its surface was distributed with unevenly sized cavities. The combustion products of EP/DCSA-Cu exhibit large and intact char layers, indicating that the charring process of the EP matrix is improved with the addition of DCSA-Cu. During polymer combustion, an integrated carbon layer with a highly graphitized structure acts as a blocking agent, thereby inhibiting the transport of heat and breakdown processes. In order to further analyze the elemental composition of the surface of the residual carbon formed after the combustion of the composite, it was tested by SEM and EDS, as shown in

https://doi.org/10.1021/acsomega.2c08226
ACS Omega 2023, 8, 16080−16093

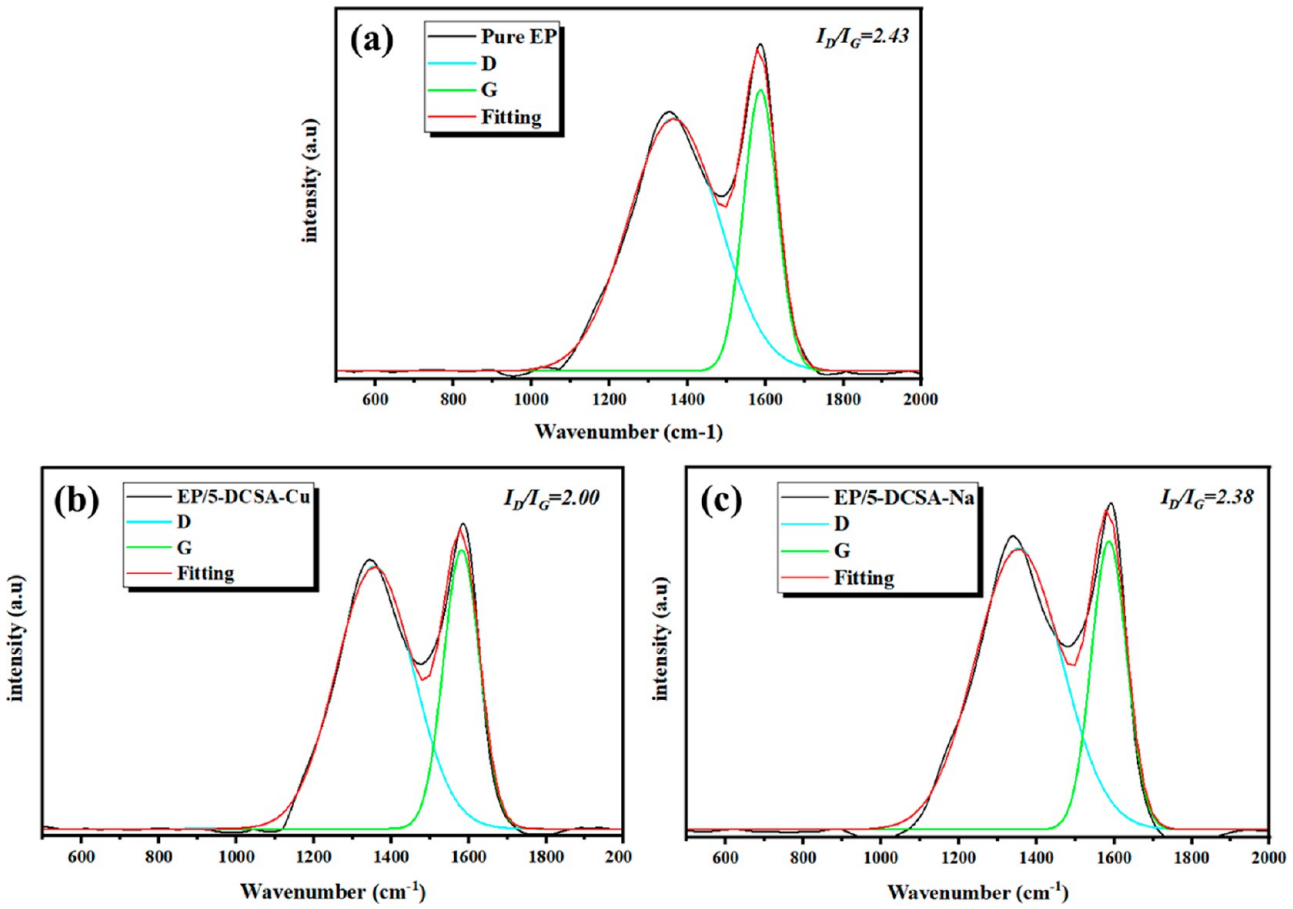

Figure 10. Raman spectra of the residue char after CCT. Pure EP (a); EP/5-DCSA-Cu (b); and EP/5-DCSA-Na (c).

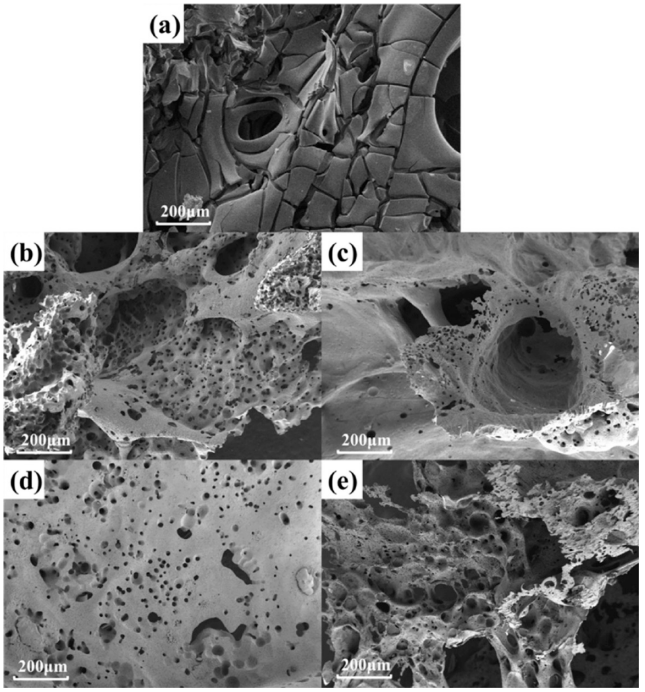

Figure 11. SEM images of char residues from CCT. Pure EP (a); EP/3-DCSA-Cu (b); EP/5-DCSA-Cu (c); EP/7-DCSA-Cu (d); and EP/5-DCSA-Na (e).

Figure 12, and the presence of metallic copper elements on the surface of the residual carbon proves that Cu^{2+} plays an active role in the catalytic carbon formation process.

3.8. Mechanisms of the DCSA-Cu Flame-Retard EP Thermoset. The flame-retardant mechanism of EP/DCSA-Cu composites is as follows in Figure 13. In the presence of a heat supply, EP can fully occupy the heat and release a large number of degradation products. A large amount of heat, smoke, and toxic CO generated continuously increases the potential fire hazard of EP. The addition of DCSA-Cu has suppressed heat, smoke, and carbon dioxide emissions, which may be attributed to the following reasons. Phosphorus compounds produced by DOPO have been reported to react with active free radicals to inhibit the growth of the flame, and therefore, less heat is transmitted to the area of degradation.

The CuO generated by Cu^{2+} is coated on the surface of the carbon layer, and the cross-linking reaction of double bonds makes the macromolecular chain and EP denser, which has a well-blocking property, which further prevents the transfer of heat and the breakdown products. Meanwhile, CuO also efficiently catalyzes the conversion of CO. Thus, EP/DCSA-Cu is inhibited from releasing heat, organic products, and CO, so that the flame retardant is increased, and smoke emission is suppressed.

3.9. Mechanical Properties of the EP Composites. The effect of cross-linking degree of flame retardants on mechanical properties was evaluated by bending and tensile experiments. The results are shown in Figure 14 and Table 5.

https://doi.org/10.1021/acsomega.2c08226
ACS Omega 2023, 8, 16080−16093

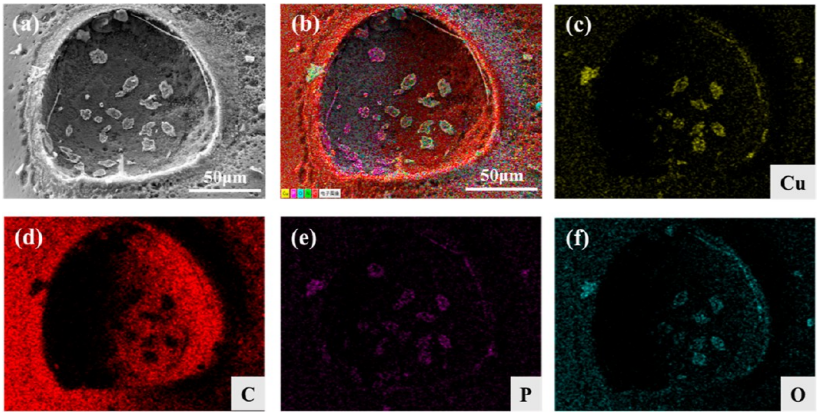

Figure 12. SEM image of carbon residues of EP/DCSA-Cu composites (a); EDS delamination images of carbon residues in EP/DCSA-Cu composites (b) and corresponding elements mapping of Cu(c), C(d), P(e), and O(f).

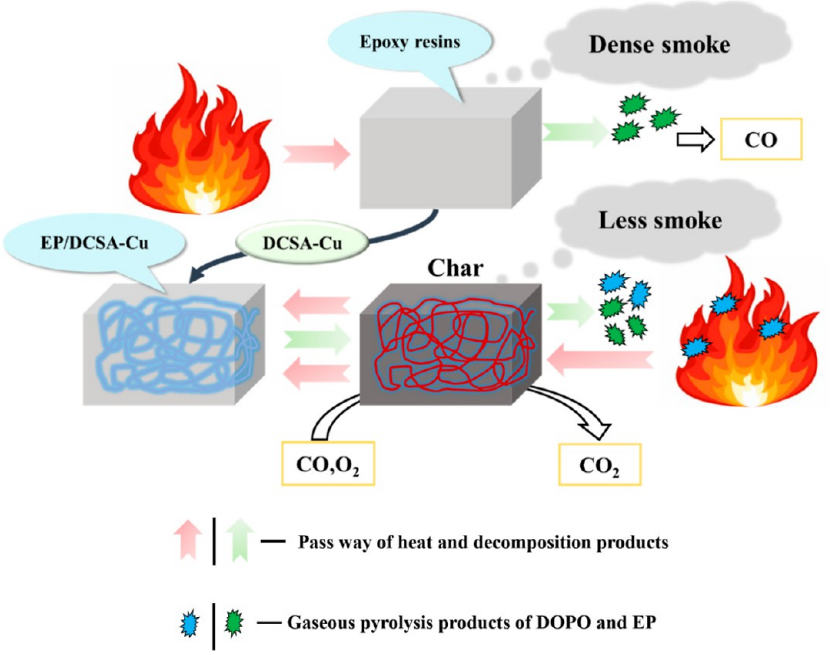

Figure 13. Schematic illustration for the mechanisms of flame retardancy.

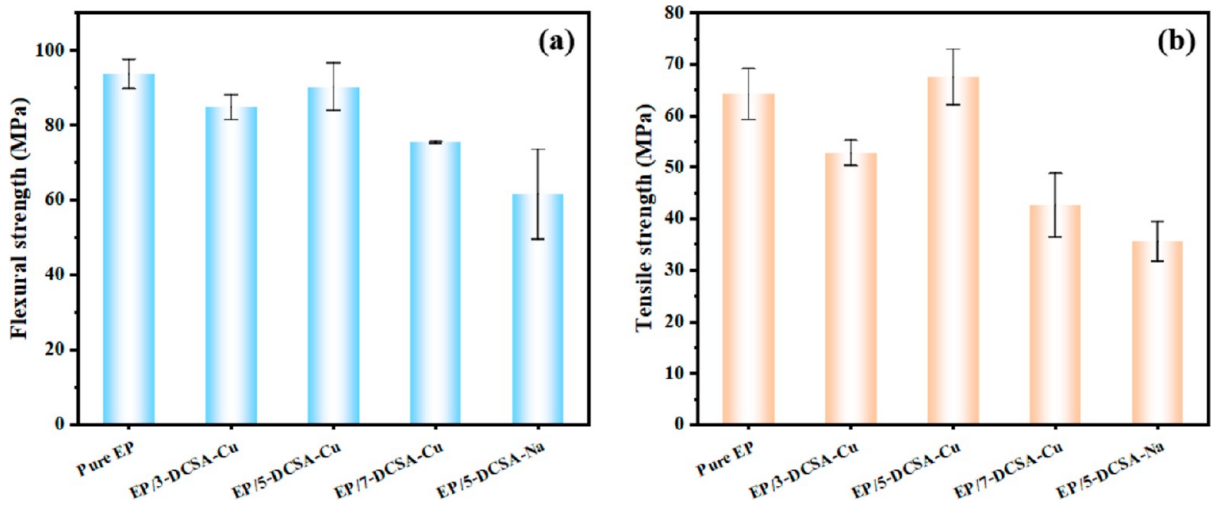

Figure 14. Flexural strength (a) and tensile strength (b) of EP composites.

https://doi.org/10.1021/acsomega.2c08226
ACS Omega 2023, 8, 16080−16093

Table 5. Mechanical Test of Neat EP and EP Composites

sample	flexural strength (MPa)	flexural modulus (GPa)	tensile strength (MPa)	tensile modulus (GPa)
pure EP	93.68	3102.20	64.17	908.37
EP/3-DCSA-Cu	84.73	2993.38	52.77	793.88
EP/5-DCSA-Cu	90.26	3684.34	67.52	928.42
EP/7-DCSA-Cu	75.36	2965.80	42.60	563.82
EP/5-DCSA-Na	61.54	3037.75	35.57	513.20

The tensile and flexural strengths of the EP/DCSA-Cu group show a decreasing trend except for 5 wt %, the decrease being due to the decrease in cross-link density brought about by the addition of flame retardants. Interestingly, the mechanical properties of the EP/5-DCSA-Cu material are maintained and even improved, probably due to the bridging effect of Cu^{2+} in DCSA-Cu between the molecular chains formed, making them more entangled. However, as the amount added increases, intermolecular agglomerates are formed resulting in weaker intermolecular chain entanglement. In particular, EP/5-DCSA-Na decreases most severely because Na^{+} only forms a single long chain molecular structure and has no effect on the intermolecular chains.

Based on the above analysis, the formation of the original macromolecular chain of DCSA-Cu molecules and the bridging effect of Cu^{2+} positively affect the mechanical properties of the EP composites.

4. CONCLUSIONS

In this study, a P/N/S−Cu^{2+}-type flame retardant material with cross-linked properties was developed successfully. In cooperation with DOPO, Cu^{2+} effectively improves the flame-retardant efficiency and safeness of EP composites. With the incorporation of 5% DCSA-Cu, EP/5-DCSA-Cu can meet the requirements of UL-94 V-0, and the LOI of EP/5-DCSA-Cu reaches 36%. The PHRR and TSP values of EP composites decreased significantly. Interestingly, DCSA-Cu was also effective in improving the heat resistance, flame retardancy, inhibition, and CO emission of the EP matrix. The results show that DOPO and Cu^{2+} have a cooperative effect on the fire safety of EP. Furthermore, 5 wt % loading of DCSA-Cu can maintain the mechanical properties of EP composites.

The flame-retardant principle of DCSA-Cu was investigated by SEM and TG-IR means. We found that DCSA-Cu was mainly involved in the quenching of free radicals. Moreover, the catalytic carbon formation of Cu^{2+} acts as a flame-retardant in the condensed phase and also catalyzes the conversion of toxic gases. We believe that the introduction of organometallic ions into halogen-free flame retardants is expected to have practical applications in flame retardancy.

AUTHOR INFORMATION

Corresponding Authors

Penglun Zheng − *College of Civil Aviation Safety Engineering, Civil Aviation Flight University of China, Guanghan 618307, P. R. China; Civil Aircraft Fire Science and Safety Engineering Key Laboratory of Sichuan Province, Guanghan 618307, P. R. China;* orcid.org/0000-0002-8081-2636; Email: zhengpenglun@cafuc.edu.cn

Yun Zheng − *Key Laboratory of Optoelectronic Chemical Materials and Devices, Ministry of Education, Jianghan University, Wuhan 430056, P. R. China;* orcid.org/0000-0003-3364-0576; Email: zhengyun@jhun.edu.cn.

Quanyi Liu − *College of Civil Aviation Safety Engineering, Civil Aviation Flight University of China, Guanghan 618307, P. R. China; Civil Aircraft Fire Science and Safety Engineering Key Laboratory of Sichuan Province, Guanghan 618307, P. R. China*; Email: quanyiliu2005@cafuc.edu.cn

Authors

Junwei Li − *College of Civil Aviation Safety Engineering, Civil Aviation Flight University of China, Guanghan 618307, P. R. China; Civil Aircraft Fire Science and Safety Engineering Key Laboratory of Sichuan Province, Guanghan 618307, P. R. China*

Huaiyin Liu − *College of Civil Aviation Safety Engineering, Civil Aviation Flight University of China, Guanghan 618307, P. R. China; Civil Aircraft Fire Science and Safety Engineering Key Laboratory of Sichuan Province, Guanghan 618307, P. R. China; Key Laboratory of Optoelectronic Chemical Materials and Devices, Ministry of Education, Jianghan University, Wuhan 430056, P. R. China*

Jichang Sun − *College of Civil Aviation Safety Engineering, Civil Aviation Flight University of China, Guanghan 618307, P. R. China; Civil Aircraft Fire Science and Safety Engineering Key Laboratory of Sichuan Province, Guanghan 618307, P. R. China; Key Laboratory of Optoelectronic Chemical Materials and Devices, Ministry of Education, Jianghan University, Wuhan 430056, P. R. China*

Yawei Meng − *College of Civil Aviation Safety Engineering, Civil Aviation Flight University of China, Guanghan 618307, P. R. China; Civil Aircraft Fire Science and Safety Engineering Key Laboratory of Sichuan Province, Guanghan 618307, P. R. China*

Haihan Zhao − *College of Civil Aviation Safety Engineering, Civil Aviation Flight University of China, Guanghan 618307, P. R. China; Civil Aircraft Fire Science and Safety Engineering Key Laboratory of Sichuan Province, Guanghan 618307, P. R. China*

Jing Wu − *College of Civil Aviation Safety Engineering, Civil Aviation Flight University of China, Guanghan 618307, P. R. China; Civil Aircraft Fire Science and Safety Engineering Key Laboratory of Sichuan Province, Guanghan 618307, P. R. China*

Complete contact information is available at: https://pubs.acs.org/10.1021/acsomega.2c08226

Author Contributions

J.L.: investigation, data curation, and writing—original draft; P.Z.: supervision and funding acquisition; H.L.: formal analysis and writing—review and editing; J.S.: methodology and review; Y.M.: supervision and methodology; H.Z.: writing—review and editing; J.W.: writing—review and editing; Y.Z.: supervision; and Q.L.: supervision and funding acquisition.

Notes

The authors declare no competing financial interest.

ACKNOWLEDGMENTS

This work was financially supported by the National Natural Science Foundation of China (no. U2033206), the funding of Civil Aircraft Fire Science and Safety Engineering Key Laboratory of Sichuan Province (no. MZ2022JB01), the General Program of Civil Aviation Flight University of China

https://doi.org/10.1021/acsomega.2c08226
ACS Omega 2023, 8, 16080−16093

(grant no. J2020-111 and J2021-110), and the Study on Performance Detection Technology of Foam Extinguishing Agent for Airport (no. J2020-106).

REFERENCES

(1) Xu, Y. J.; Wang, J.; Tan, Y.; Qi, M.; Chen, L.; Wang, Y. Z. A novel and feasible approach for one-pack flame-retardant epoxy resin with long pot life and fast curing. *Chem. Eng. J.* **2018**, *337*, 30−39.
(2) Jiang, J.; Cheng, Y. B.; Liu, Y.; Wang, Q.; He, Y. S.; Wang, B. W. Intergrowth charring for flame-retardant glass fabric-reinforced epoxy resin composites. *Journal of Materials Chemistry A* **2015**, *3*, 4284−4290.
(3) Wang, X.; Hu, Y.; Song, L.; Xing, W. Y.; Lu, H. D. A. Thermal degradation mechanism of flame retarded epoxy resins with a DOPO-substituted organophosphorus oligomer by TG-FTIR and DP-MS. *J. Anal. Appl. Pyrolysis* **2011**, *92*, 164−170.
(4) Luda, M. P.; Balabanovich, A.; Camino, G.; Camino, G. Thermal decomposition of fire retardant brominated epoxy resins. *J. Anal. Appl. Pyrolysis* **2002**, *65*, 25−40.
(5) Hendriks, H. S.; Westerink, R. H. S. Neurotoxicity and risk assessment of brominated and alternative flame retardants. *Neurotoxicol. Teratol.* **2015**, *52*, 248−269.
(6) Fan, H. Z.; Zhao, J. M.; Zhang, J. F.; Li, H. F.; Zhang, S.; Sun, J.; Xin, F.; Liu, F.; Qin, Z. D.; Tang, W. F. TiO 2/SiO2/kaolinite hybrid filler to improve the flame retardancy, smoke suppression and anti-aging characteristics of epoxy resin. *Mater. Chem. Phys.* **2022**, *277*, 125576.
(7) Xie, W. Q.; Huang, S. W.; Liu, S. M.; Zhao, J. Q. Phosphorus-based triazine compound endowing epoxy thermosets with excellent flame retardancy and enhanced mechanical stiffness. *Polym. Degrad. Stab.* **2020**, *180*, 109293.
(8) Lu, L. G.; Zeng, Z. J.; Qian, X. D.; Shao, G. S.; Wang, H. Y. Thermal degradation and combustion behavior of flame-retardant epoxy resins with novel phosphorus-based flame retardants and silicon particles. *Polymer Bulletin* **2019**, *76*, 3607−3619.
(9) Lu, L. G.; Guo, N.; Qian, X. D.; Yang, S. S.; Wang, X. B.; Jin, J.; Shao, G. S. Thermal degradation and combustion behavior of intumescent flame-retardant polypropylene with novel phosphorus-based flame retardants. *J. Appl. Polym. Sci.* **2018**, *135*, 45962.
(10) Szolnoki, B.; Toldy, A.; Konrad, P.; Szebenyi, G.; Marosi, G. Comparison of additive and reactive phosphorus-based flame retardants in epoxy resins. *Periodica Polytechnica-Chemical Engineering* **2013**, *57*, 85−91.
(11) Hua, Y. F.; Sun, J.; Jiang, S. L.; Gu, X. Y.; Zhang, S. *Synthesis of a DOPO Derivative to Improve the Fire Safety and Mechanical Performance of Epoxy Resin*, 2022; Macromolecular Materials and Engineering.
(12) Xu, F.; Zhang, G. X.; Wang, P.; Dai, F. Y. A novel epsilon-polylysine-derived durable phosphorus-nitrogen-based flame retardant for cotton fabrics. *Cellulose* **2021**, *28*, 3807−3822.
(13) Chen, J. L.; Wang, J. H.; Ni, A. Q.; Chen, H. D.; Shen, P. L. Synthesis of a Novel Phosphorous-Nitrogen Based Charring Agent and Its Application in Flame-retardant HDPE/IFR Composites. *Polymers* **2019**, *11*, 1062.
(14) Kabisch, B.; Fehrenbacher, U.; Kroke, E. Hexamethoxycyclotriphosphazene as a flame retardant for polyurethane foams. *Fire Mater.* **2014**, *38*, 462−473.
(15) Wang, R. Z.; Chen, Y.; Liu, Y. Y.; Ma, M. L.; Tong, Z. Y.; Chen, X. L.; Bi, Y. X.; Huang, W. B.; Liao, Z. J.; Chen, S. L.; Zhang, X. Y.; Li, Q. Q. Metal-organic frameworks derived ZnO@MOF@PZS flame retardant for reducing fire hazards of polyurea nanocomposites. *Polym. Adv. Technol.* **2021**, *32*, 4700−4709.
(16) Yang, Z.; Guo, W. C.; Yang, P.; Hu, J. F.; Duan, G. G.; Liu, X. H.; Gu, Z. P.; Li, Y. W. Metal-phenolic network green flame retardants. *Polymer* **2021**, *221*, 123627.
(17) Huang, R.; Guo, X. Y.; Ma, S. Y.; Xie, J. X.; Xu, J. Z.; Ma, J. Novel Phosphorus-Nitrogen-Containing Ionic Liquid Modified Metal-Organic Framework as an Effective Flame Retardant for Epoxy Resin. *Polymers* **2020**, *12*, 108.
(18) Yen, Y. Y.; Wang, H. T.; Guo, W. J. Synergistic flame retardant effect of metal hydroxide and nanoclay in EVA composites. *Polym. Degrad. Stab.* **2012**, *97*, 863−869.
(19) Hu, M. Y.; Xiong, K. K.; Li, J. R.; Jing, X. B.; Zhao, P. H. Novel P/N/Si/S-containing Mononickel Complex as a Metal-based Intumescent Flame Retardant for Cotton Fabrics. *Fibers and Polymers* **2019**, *20*, 1794−1802.
(20) Chen, Y. J.; Xu, L. F.; Wu, X. D.; Xu, B. The influence of nano ZnO coated by phosphazene/triazine bi-group molecular on the flame retardant property and mechanical property of intumescent flame retardant poly (lactic acid) composites. *Thermochim. Acta* **2019**, *679*, 178336.
(21) Zheng, Y.; Lu, Y. S.; Zhou, K. Q. A novel exploration of metal-organic frameworks in flame-retardant epoxy composites. *J. Therm. Anal. Calorim.* **2019**, *138*, 905−914.
(22) Xu, W. Z.; Fan, L. J.; Qin, Z. Q.; Liu, Y. C.; Li, M. Silica-coated metal-organic framework-beta-FeOOH hybrid for improving the flame retardant and smoke suppressive properties of epoxy resin. *Plastics Rubber and Composites* **2021**, *50*, 396−405.
(23) Wang, H. W.; Qiao, H.; Guo, J.; Sun, J.; Li, H. F.; Zhang, S.; Gu, X. Y. Preparation of cobalt-based metal organic framework and its application as synergistic flame retardant in thermoplastic polyurethane (TPU). *Composites Part B-Engineering* **2020**, *182*, 107498.
(24) Cai, W.; Guo, W. W.; Pan, Y.; Wang, J. L.; Mu, X. W.; Feng, X. M.; Yuan, B. H.; Wang, B. B.; Hu, Y. Polydopamine-bridged synthesis of ternary h-BN@PDA@SnO2 as nanoenhancers for flame retardant and smoke suppression of epoxy composites. *Composites Part a-Applied Science and Manufacturing* **2018**, *111*, 94−105.
(25) Chen, X. L.; Chen, X. H.; Li, S. X.; Jiao, C. A. M. Copper metal-organic framework toward flame-retardant enhancement of thermoplastic polyurethane elastomer composites based on ammonium polyphosphate. *Polym. Adv. Technol.* **2021**, *32*, 2829−2842.
(26) Yuan, Y.; Wang, W.; Xiao, Y.; Chun Yin Yuen, A.; Mao, L.; Pan, H.; Yu, B.; Hu, Y. Surface modification of multi-scale cuprous oxide with tunable catalytic activity towards toxic fumes and smoke suppression of rigid polyurethane foam. *Appl. Surf. Sci.* **2021**, *556*, 149792.
(27) Xu, Z.; Xing, W.; Hou, Y.; Zou, B.; Han, L.; Hu, W.; Hu, Y. The combustion and pyrolysis process of flame-retardant polystyrene/cobalt-based metal organic frameworks (MOF) nanocomposite. *Combust. Flame* **2021**, *226*, 108−116.
(28) Peng, X.; Li, Z.; Wang, D.; Li, Z.; Liu, C.; Wang, R.; Jiang, L.; Liu, Q.; Zheng, P. A facile crosslinking strategy endows the traditional additive flame retardant with enormous flame retardancy improvement. *Chem. Eng. J.* **2021**, *424*, 130404.
(29) Peng, X.; Liu, Q.; Wang, D.; Liu, C.; Zhao, Y.; Wang, R.; Zheng, P. A hyperbranched structure formed by in-situ crosslinking of additive flame retardant endows epoxy resins with great flame retardancy improvement. *Composites, Part B* **2021**, *224*, 109162.
(30) Wang, D.; Liu, Q.; Peng, X.; Liu, C.; Li, Z.; Li, Z.; Wang, R.; Zheng, P.; Zhang, H. High-efficiency phosphorus/nitrogen-containing flame retardant on epoxy resin. *Polym. Degrad. Stab.* **2021**, *187*, 109544.
(31) Chen, M.; Lin, X.; Liu, C.; Zhang, H. An effective strategy to enhance the flame retardancy and mechanical properties of epoxy resin by using hyperbranched flame retardant. *J. Mater. Sci.* **2021**, *56*, 5956−5974.
(32) Zhang, J.; Mi, X.; Chen, S.; Xu, Z.; Zhang, D.; Miao, M.; Wang, J. A bio-based hyperbranched flame retardant for epoxy resins. *Chem. Eng. J.* **2020**, *381*, 122719.
(33) Buczko, A.; Stelzig, T.; Bommer, L.; Rentsch, D.; Heneczkowski, M.; Gaan, S. Bridged DOPO derivatives as flame retardants for PA6. *Polym. Degrad. Stab.* **2014**, *107*, 158−165.
(34) Zhang, W. C.; Li, X. M.; Yang, R. J. Novel flame retardancy effects of DOPO-POSS on epoxy resins. *Polym. Degrad. Stab.* **2011**, *96*, 2167−2173.

https://doi.org/10.1021/acsomega.2c08226
ACS Omega 2023, 8, 16080−16093

(35) Xiu, F. R.; Weng, H. W.; Qi, Y. Y.; Yu, G. D.; Zhang, Z. G.; Zhang, F. S. A novel reutilization method for waste printed circuit boards as flame retardant and smoke suppressant for poly (vinyl chloride). *J. Hazard. Mater.* **2016**, *315*, 102−109.
(36) Zhang, W. Y.; Zhang, W. C.; Pan, Y. T.; Yang, R. J. Facile synthesis of transition metal containing polyhedral oligomeric silsesquioxane complexes with mesoporous structures and their applications in reducing fire hazards, enhancing mechanical and dielectric properties of epoxy composites. *J. Hazard. Mater.* **2021**, *2021*, 401.
(37) Xiao, Y. L.; Ma, C.; Jin, Z. Y.; Wang, J. L.; He, L. X.; Mu, X. W.; Song, L.; Hu, Y. Functional covalent organic framework for exceptional Fe2+, Co(2+)and Ni2+ removal: An upcycling strategy to achieve water decontamination and reutilization as smoke suppressant and flame retardant simultaneously. *Chem. Eng. J.* **2021**, *421*, 127837.
(38) Song, K.; Hou, B.; Rehman, Z. U.; Pan, Y.-T.; He, J. Y.; Wang, D.-Y.; Yang, R. J. Sloughing of metal-organic framework retaining nanodots via step-by-step carving and its flame-retardant effect in epoxy resin. *Chem. Eng. J.* **2022**, *448*, 137666.

https://doi.org/10.1021/acsomega.2c08226
ACS Omega 2023, 8, 16080−16093